Research Square

Preprints are preliminary reports that have not undergone peer review.
They should not be considered conclusive, used to inform clinical practice,
or referenced by the media as validated information.

Reduced flip angle improves vertebral artery V3 depiction without compromising other cervical vessels in 3D TOF MRA

Guijin Li
Beijing Chao-Yang Hospital, Capital Medical University
Jiewen Qiu
Tingzhou Hospital
Dianjiang Zhao
Beijing Chao-Yang Hospital, Capital Medical University
Hongjie Cao
Beijing Chao-Yang Hospital, Capital Medical University
Xiuqin Jia
Beijing Chao-Yang Hospital, Capital Medical University
Haishui Xie
Tingzhou Hospital
Shuitao Qiu
Tingzhou Hospital
Qi Yang
yangyangqiqi@gmail.com

Beijing Chao-Yang Hospital, Capital Medical University

Research Article

Keywords: Magnetic resonance angiography, Vertebral artery, Flip angle, Time-of-flight, Image quality

Posted Date: November 27th, 2026

DOI: https://doi.org/10.21203/rs.3.rs-11622412/v1

License: This work is licensed under a Creative Commons Attribution 4.0 International License.
Read Full License

Additional Declarations: No competing interests reported.

Abstract

Background

To identify the optimal flip angle (FA) for depicting the slow-flow vertebral artery V3 segment on cervical 3D time-of-flight MRA (3D TOF-MRA) without degrading other cervical vessels.

Materials and methods

In a prospective single-centre study, 30 participants (19 women; mean age 52.4 ± 10.6 years) underwent cervical 3D TOF-MRA at eight FAs (8–25°; 18° routine; TONE 70%, 3 T). SNR, CNR, CBR, the V3/ICA-C3 signal ratio and proximal-to-distal V3 decay were measured; two radiologists scored V3, ICA-C3, V2 and common carotid origin depiction (5-point) and diagnostic adequacy. Repeated-measures ANOVA, Friedman and Wilcoxon (reference 18°) with Bonferroni correction were used.

Results

The V3 score peaked at 12° (4.78 ± 0.51); diagnostic adequacy was 100% at 10° and 12° but only 43.3% at 18° ($p < 0.001$). ICA-C3, common carotid origin and V2 signals rose monotonically with FA and were only mildly lower at 12° than at 18°, without V3-like saturation decline.

Conclusions

The optimal FA for V3 is 12° (10–14° acceptable), well below the routine 18°. Lowering the FA to 12° improved V3 depiction without significant loss of other-vessel depiction, despite mild SNR/CNR reduction, consistent with the blood Ernst angle for slow flow.

Background

The carotid and vertebral arteries are the principal supply routes to the brain, and dissection, stenosis and tortuosity of these vessels are important causes of ischemic stroke [1] [2]. Accurate assessment of their morphology and lumen is therefore central to diagnosis, treatment planning and follow-up [3] [4]. Catheter digital subtraction angiography (DSA) remains the golden standard but is invasive, costly and associated with ionizing radiation [5]. Three-dimensional time-of-flight MR angiography (3D TOF-MRA) relies on flow-related enhancement to depict the cervical arteries without exogenous contrast or ionizing radiation; it is well suited to screening for steno-occlusive disease and to evaluating vascular malformations [6].

Cervical TOF-MRA nevertheless has technical limitations. Turbulence at tortuous, bifurcating or stenotic segments causes signal loss that may exaggerate stenosis, and slow or in-plane flow is readily

saturated, weakening depiction of distal, collateral and slow-flow vessels; a large coverage volume further increases slice thickness, acquisition time and susceptibility to motion, fat or dental-metal artefacts [6] [7]. Among the adjustable parameters, the excitation flip angle (FA) is pivotal because it simultaneously determines inflow enhancement and background suppression: a small FA yields insufficient blood signal, whereas an excessive FA accelerates saturation, particularly in slow-flow or tortuous segments [7] [8] .

Prior work optimized variable flip angles for cervical TOF-MRA via TONE (e.g., Nägele et al. 1994; Atkinson et al. 1994; Ikushima et al. 1997), but the flip angle required by the slow-flow, tortuous V3 segment — and whether its optimum degrades the remaining cervical vessels — has not been systematically quantified. Because the V3 segment is tortuous with comparatively slow flow, its FA requirement likely differs from that of the fast-flow carotid system for which cervical protocols are configured; whether tailoring the FA to V3 affects the remaining cervical vessels is also unclear [9–14]. We therefore prospectively compared eight TONE centre FAs using quantitative (SNR, CNR, CBR, V3-to-ICA-C3 signal ratio and proximal-to-distal signal decay) and qualitative (5-point scoring) endpoints, to identify the optimal centre FA for V3 and test whether it degrades depiction of other vessels.

Materials and methods

Study population

This single centre prospective study was approved by the Institutional Review Board of Tingzhou Hospital (approval No. TZYY-2026-0413), and written informed consent was obtained from all participants. All procedures were performed in accordance with the ethical standards of the institutional and national research committees and with the 1964 Declaration of Helsinki and its later amendments. The study is reported in accordance with the STROBE statement for observational studies [15].

Between November 2025 and July 2026, a total of 289 patients underwent cervical TOF-MRA; 43 consented to the additional prospective multi-FA protocol. 2 patients were excluded for prior cervical stent or vascular surgery and 11 for incomplete acquisitions or non-diagnostic image quality. The final cohort comprised 30 participants who completed all eight FAs acquisitions (Fig. 1). Inclusion criteria were age ≥ 18 years, no MRI contraindication, clinical suspicion of intracranial ischemia or cervical carotid/vertebral artery disease, written consent, and adequate cooperation for repeated scanning. Exclusion criteria were prior cervical stent or vascular surgery, inability to complete all FAs acquisitions or non-diagnostic image quality, and any absolute MRI contraindication.

Image acquisition

Imaging was performed on a 3.0T system (i_Space 3.0T Pro, Wandong Medical Equipment Co., Ltd, Beijing, China) with a head-neck phased array coil. Each participant underwent 3D TOF-MRA acquisition with 8 different FAs; all other parameters were identical: repetition time TR=22ms; echo time TE =

3.69ms; field of view = 230 × 230 mm; matrix = 256 × 225; slice thickness = 1.0mm; voxel size = 0.9 × 1.0 × 1.0 mm^3; average = 1; parallel imaging factor = 2; bandwidth=250kHz; TONE (the ratio of the FA at the slab inflow end to that at the outflow end [13, 14] [16–20]) = 70%, i.e. the FA increases linearly from the inflow to the outflow end of the slab (for example, from 9.9° at the inflow end to 14.1° at the outflow end at the centre FA of 12°); and acquisition time=5min11s per FA. In this study, the FA was defined as the TONE centre FA, and the following values were used: 8°, 10°, 12°, 14°, 16°, 18° (routine), 20°, and 25°. FA order was randomized. Coverage extended from the upper margin of the aortic arch to the circle of Willis, with a saturation band to suppress venous signal.

Image analysis

Qualitative analysis

Images were anonymized as to FA and loaded onto a post-processing workstation (Syngo Via VB80, Siemens Healthineers, Erlangen, Germany). Two board-certified radiologists (with 15 and 6 years of cardiovascular MRI experience) independently assessed overall image quality and the depiction of the vertebral artery V2 and V3 segment, internal carotid artery (ICA) C3 segment and common carotid artery origin on a standardized 5-point scale under blind conditions. Discrepancies were resolved by consensus after standardized training. For overall quality, the scale was 1 = multiple segments invisible, or non-diagnostic; 2 = partially visible with marked signal loss in several segments; 3 = essentially visible with slightly reduced signal in some segments; 4 = fully visible with good overall signal; and 5 = fully visible with uniform signal and excellent background suppression. For each vessel segment, the scale was 1 = not visible; 2 = partially visible; 3 = visible but clearly lower in signal than other segments; 4 = visible but slightly lower in signal than other segments; and 5 = visible with signal equal to that of other segments.

Quantitative analysis

A third board-certified radiologist (8 years of cardiovascular MRI experience) placed circular regions of interest (ROIs) on the left and right V3 segments, on muscle in the same phase-encoding direction and on background air, and on the left and right ICA C3 segments. ROIs were sized to one-half to two-thirds of the vessel diameter and avoided the vessel wall and plaque; the noise ROI was placed in air outside the anatomical in the phase-encoding direction to avoid pulsation and fat signal. The following metrics were derived: SNR=blood signal intensity (SI) / background SD; CNR= (blood SI − muscle SI) / background SD; CBR= (blood SI − muscle SI) / muscle SI, which is noise-independent [21]; the V3/ICA-C3 signal ratio=V3 SI / ipsilateral ICA-C3 SI, cancelling individual differences in flow and coil sensitivity; and the proximal-to-distal signal decay rate = (proximal SI − distal SI) / proximal SI × 100%, quantifying signal continuity along the segment. V3 score ≥ 4 defined reader-assessed diagnostic adequacy (a surrogate for interpretability, not diagnostic accuracy against an independent reference standard such as DSA or CE-MRA); a side with zero V3 signal at all eight FAs and rated completely invisible by both readers was recorded as non-visualized and treated as missing without imputation.

Statistical analysis

All analyses used IBM SPSS Statistics 26.0 (IBM Corp.). Normally distributed data are mean ± SD. Continuous variables across the eight FAs were compared with repeated-measures ANOVA (Greenhouse–Geisser correction) for normally distributed data and the Friedman test otherwise; pairwise comparisons against 18° used the Wilcoxon signed-rank test with Bonferroni correction. Categorical variables were compared with chi-square or Fisher's exact test. Inter-reader agreement for qualitative scores was assessed with weighted kappa. Two-sided $p < 0.05$ denoted statistical significance.

Results

Of all 289 screened subjects, 43 consented and 30 (11 men and 19 women; mean age 52.4 ± 10.6 years, range 33–79 years) completed all eight FAs acquisitions and formed the final cohort (Fig. 1); baseline characteristics are summarized in Table 1. Vertebral artery dominance was balanced in 22 participants, left-dominant in 6 and right-dominant in 2. One side of one participant was non-visualized at all FAs and was treated as missing.

Table 1
Baseline characteristics of the study cohort (*n* = 30).

Characteristic	Value
Age (years), mean ± SD	52.4 ± 10.6
Age range (years)	33–79
Male, n (%)	11 (36.7)
Female, n (%)	19 (63.3)
Vertebral artery dominance, balanced, n (%)	22 (73.3)
Vertebral artery dominance, left-dominant, n (%)	6 (20.0)
Vertebral artery dominance, right-dominant, n (%)	2 (6.7)
Enrolment period	November 2025 – July 2026

SD, standard deviation. Vertebral artery dominance indicates the side supplying the larger calibers/flow. One participant was non-visualized at all FAs and treated as missing in the dominance-stratified analyses. The enrolment period is shown as reported in the study protocol.

Qualitative results

Inter-reader agreement was good to excellent. For V3 depiction the weighted kappa was 0.984 (95% confidence interval [CI], 0.974–0.991) on the left and 0.983 (95% CI, 0.974–0.990) on the right; all remaining items had kappa ≥ 0.80.

V3 scores differed significantly across the eight FAs (Friedman $\chi^2 = 180.15$, $p < 0.001$, Kendall's W = 0.858). The peak was at 12° (4.78 ± 0.51), with 10° (4.71 ± 0.62) and 14° (4.58 ± 0.65) performing similarly; scores fell appreciably from 16° and reached 1.39 ± 0.54 at 25° (Table 2, Fig. 2a). Reader-assessed diagnostic adequacy was 100% at 10° and 12° but fell to 43.3% at 18° and 1.7% at 25°; the 95% CI of the mean V3 score was 4.59–4.97 at 12° and 2.88–3.46 at 18° (n = 30), and reader-assessed diagnostic adequacy was 100% (95% CI 88.4–100%) at 12° versus 43.3% (95% CI 25.9–62.6%) at 18°.

Table 2
Reader-assessed depiction scores (mean ± SD) of the cervical segments and V3 diagnostic adequacy at each FA (n = 30).

Flip angle	V3 visual score (mean ± SD)	V3 diagnostic adequacy (%)	ICA-C3 score (mean ± SD)	V2 score (mean ± SD)	CCA origin score (mean ± SD)
8°	3.92 ± 0.58	70.0	3.65 ± 0.40	3.71 ± 0.46	3.37 ± 0.41
10°	4.71 ± 0.62	100.0	4.52 ± 0.40	4.58 ± 0.50	4.26 ± 0.45
12°	4.78 ± 0.51	100.0	4.97 ± 0.10	4.93 ± 0.26	4.91 ± 0.30
14°	4.58 ± 0.65	96.7	4.98 ± 0.09	4.93 ± 0.26	4.97 ± 0.14
16°	3.91 ± 0.70	73.3	4.99 ± 0.05	4.93 ± 0.26	4.97 ± 0.14
18°	3.17 ± 0.77	43.3	5.00 ± 0.00	4.92 ± 0.29	4.97 ± 0.14
20°	2.29 ± 0.68	8.3	5.00 ± 0.00	4.86 ± 0.43	4.98 ± 0.09
25°	1.39 ± 0.54	1.7	5.00 ± 0.00	4.79 ± 0.53	4.98 ± 0.09

Scores are the mean of two readers. Diagnostic adequacy is the mean proportion, per participant (n = 30), judged diagnostic by the two readers, with a V3 score ≥ 4 defining reader-assessed diagnostic adequacy. SD, standard deviation. The internal carotid artery C3, vertebral artery V2 and common carotid artery origin depiction scores were likewise averaged across the two readers and left/right sides and are reported on the same 1–5 scale.

Relative to the routine 18°, V3 scores at 8–16° were all significantly higher (Bonferroni-corrected $p < 0.05$), with the largest difference at 12° (+ 1.61), whereas 20° and 25° were significantly lower (− 0.88 and − 1.78, respectively; $p < 0.05$) (Table 3).

Table 3
Comparison of the V3 segment visual score at each FA with the routine 18° reference (Wilcoxon signed-rank test, *n* = 30).

Flip angle	Mean V3 score	Difference vs 18°	*Z*	*p*	Bonferroni-corrected *p*	Significant
8°	3.925	+ 0.758	−3.29	0.001	0.007	Yes
10°	4.708	+ 1.542	−4.25	< 0.001	< 0.001	Yes
12°	4.775	+ 1.608	−4.26	< 0.001	< 0.001	Yes
14°	4.583	+ 1.417	−4.29	< 0.001	< 0.001	Yes
16°	3.908	+ 0.742	−4.33	< 0.001	< 0.001	Yes
20°	2.292	−0.875	−4.55	< 0.001	< 0.001	Yes
25°	1.392	−1.775	−4.49	< 0.001	< 0.001	Yes

The mean reference score at 18° was 3.167. Bonferroni correction was the raw $p \times 7$, and a corrected $p < 0.05$ was taken to indicate significance.

Representative MIP images of the cervical vessels at 12° and 18° are shown in Fig. 3. At the lower FA, the vertebral artery V3 segment (orange arrow) is depicted more completely and with less in-slab signal loss than at the routine 18°, a visual impression that mirrors the higher V3 visual score and reader-assessed diagnostic adequacy at 12° reported above.

Depiction of the other cervical segments (ICA-C3, common carotid origin and vertebral artery V2) across the eight flip angles is summarized in Table 2 (n = 30; scores averaged across readers and sides). All three segments scored near the ceiling of the 5-point scale from 10° to 25°; at 12° the mean scores were 4.91 ± 0.30 (CCA origin), 4.97 ± 0.10 (ICA-C3) and 4.93 ± 0.26 (V2), essentially identical to the 18° values (4.97 ± 0.14, 5.00 ± 0.00 and 4.92 ± 0.29).

Compared with the routine 18° flip angle, lowering the FA to 12° changed reader-assessed depiction of the other cervical segments only negligibly (paired mean difference 12°−18°): CCA origin − 0.07 ± 0.19 (95% CI − 0.14 to + 0.00), ICA-C3 − 0.03 ± 0.10 (95% CI − 0.06 to + 0.01), and V2 + 0.01 ± 0.05 (95% CI − 0.01 to + 0.03). All 95% confidence intervals spanned zero, and the one-sided 95% lower bounds (− 0.12, − 0.06, and − 0.01) exceeded a − 0.5 non-inferiority margin, confirming that the 12° protocol cause no significant loss in reader-assessed depiction of these segments.

Depiction of the other cervical segments behaved differently: their SNR and CNR increased monotonically with FA and peaked only at 25°, and at 12° these values were mildly lower than at 18° (e.g. ICA-C3 SNR, 389.3 ± 83.4 vs 504.2 ± 111.4) but remained high, showing no saturation-driven decline like V3 (Table 4, Fig. 5).

Table 4
Quantitative metrics of the other cervical segments at each FA (n = 30).

Flip angle	ICA-C3 SNR	ICA-C3 CNR	V2 SNR	Common carotid artery origin SNR
8°	289.2 ± 77.1	140.3 ± 44.1	305.3 ± 78.8	257.6 ± 69.8
10°	343.5 ± 88.0	192.3 ± 57.1	356.0 ± 91.2	297.8 ± 84.2
12°	389.3 ± 83.4	241.4 ± 60.0	402.3 ± 78.9	332.6 ± 79.1
14°	427.3 ± 101.4	288.2 ± 73.1	416.5 ± 100.1	354.2 ± 92.6
16°	461.5 ± 85.7	331.6 ± 67.8	451.9 ± 90.0	373.9 ± 70.8
18°	504.2 ± 111.4	376.1 ± 89.0	475.8 ± 107.0	408.2 ± 88.9
20°	536.0 ± 135.8	416.0 ± 111.0	479.6 ± 112.7	424.8 ± 115.1
25°	584.5 ± 136.4	477.7 ± 113.8	498.7 ± 120.8	462.2 ± 132.3

Data are mean ± SD. SNR, signal-to-noise ratio; CNR, contrast-to-noise ratio; ICA, internal carotid artery; V2, vertebral artery V2 segment. Both ratios are dimensionless. The metrics increase monotonically with FA, peaking at 25°; values at 12° are lower than at 18° but remain high. Data is from the same cohort of 30 participants as Tables 2 and 5.

Quantitative results

All quantitative metrics differed significantly across the eight FAs (Greenhouse–Geisser-corrected $p < 0.001$), the strongest FA effects being the proximal-to-distal decay rate ($F = 283.16$) and the V3/ICA-C3 signal ratio (Table 5, Fig. 4). V3 SNR described an inverted U, rising from 333.1 ± 94.8 at 8° to a plateau of ~ 430 between 14° and 18° and falling to 358.5 ± 93.0 at 25°. V3 CNR peaked at 18° (302.5 ± 86.7), whereas V3 CBR increased monotonically to 2.50 ± 0.78 at 20°. In contrast, the V3/ICA-C3 signal ratio decreased monotonically from 1.16 ± 0.13 at 8° to 0.62 ± 0.15 at 25°, and the proximal-to-distal decay rate increased monotonically from 7.37% ± 6.87% to 50.18% ± 9.44%.

Table 5
Quantitative metrics of the vertebral artery V3 segment at each FA (*n* = 30).

Flip angle	V3 SNR	V3 CNR	V3 CBR	V3/ICA-C3 signal ratio	V3 proximal-to-distal decay rate (%)
8°	333.1 ± 94.8	184.2 ± 59.5	1.23 ± 0.19	1.16 ± 0.13	7.37 ± 6.87
10°	388.2 ± 92.0	237.1 ± 59.8	1.58 ± 0.22	1.14 ± 0.13	14.55 ± 6.64
12°	417.5 ± 84.5	269.4 ± 61.0	1.83 ± 0.30	1.09 ± 0.15	17.42 ± 6.78
14°	430.6 ± 111.7	291.6 ± 84.8	2.11 ± 0.42	1.01 ± 0.15	25.08 ± 7.54
16°	429.7 ± 85.0	299.8 ± 69.8	2.34 ± 0.52	0.94 ± 0.16	30.06 ± 7.66
18°	430.2 ± 102.7	302.5 ± 86.7	2.42 ± 0.71	0.86 ± 0.16	36.72 ± 8.28
20°	417.0 ± 121.5	297.1 ± 102.2	2.50 ± 0.78	0.78 ± 0.16	40.68 ± 8.56
25°	358.5 ± 93.0	251.9 ± 84.4	2.46 ± 0.96	0.62 ± 0.15	50.18 ± 9.44
F value	9.79	20.60	48.89	199.50	283.16
p (Greenhouse–Geisser)	< 0.001	< 0.001	< 0.001	< 0.001	< 0.001
Partial η^2	0.252	0.415	0.628	0.873	0.907

Data are mean ± SD and were analyzed with one-way repeated-measures analysis of variance (df1 = 7, df2 = 203). The *F* value and partial eta squared (η^2) quantify the effect of FA across the eight levels; partial η^2 ranges from 0 to 1 and the larger values for the decay rate and the V3/ICA-C3 signal ratio indicate the strongest flip-angle dependence. CBR, contrast-to-background ratio; CNR, contrast-to-noise ratio; ICA, internal carotid artery; SNR, signal-to-noise ratio. All ratios are dimensionless and the decay rate is a percentage.

Vertebral artery dominance subgroup

Among the 8 dominant-type participants (7 with both sides evaluable), the dominant side showed higher V3 signal intensity (+ 191.6), SNR (+ 100.9) and CNR (+ 96.5) than the non-dominant side (all p = 0.047). The non-dominant side tolerated high FAs less well, with an earlier peak in its score curve, and the FA × side interaction was significant for CNR (p = 0.043) and CBR (p = 0.019). Because of the small subgroup size, these findings are exploratory.

Discussion

This study shows that in this single-centre 3T setting with TONE 70%, the optimal TONE centre FA for the vertebral artery V3 segment on cervical 3D TOF-MRA is 12° (10–14° acceptable), markedly below the routine 18°; across 8–16° both V3 scores and adequacy exceeded those at 18°. This gain degraded no other cervical vessel, indicating that the FA optimized for the fast-flow carotid system is systematically too large for V3.

The optimal TOF FA depends on flow velocity, vessel orientation and transit time [12–14]. In fast-flow, largely through-plane vessels such as the ICA and basilar artery, blood protons are replaced within a single TR and accumulate little saturation, so a larger FA both suppresses stationary background and increases vessel-to-background contrast. Consequently, 3D TOF-MRA protocols for these targets and most presets use an FA of about 18–20° [12–14] [22, 23] and do not transfer to the slow-flow, tortuous V3 segment;

A larger FA converts longitudinal into transverse magnetization, increasing signal, but under short TR it also drives slow-flow protons within the slab toward saturation. For fast-flow vessels these effects are compatible; for V3, the steady-state signal depends on the Ernst angle ($\alpha E = \arccos[\exp(-TR/T1)]$) [24–26]; with TR 22 ms and blood T1 ≈ 1500–2000 ms at 3.0T [24, 27], the Ernst angle is about 9–10° [22, 23]. Fast flow escapes saturation by traversing the slab quickly, whereas in slow, in-plane V3 an excessive angle prematurely exhausts longitudinal magnetization, appearing as pseudo-stenosis or pseudo-occlusion. Reducing the FA to 10–14° returns it toward the blood Ernst angle, preserving V3 signal while still suppressing stationary tissue.

In this study, V3 SNR peaked at 14–18° and CNR at 18°, whereas the subjective score peaked at 12° and reader-assessed diagnostic adequacy had already fallen to 43.3% at 18°. This divergence shows that peak SNR or CNR alone can mislead, because they average signal over an ROI and cannot capture along-segment non-uniformity. As FA increases, the proximal V3 may retain high signal while the distal portion decays, so the segment appears interrupted or falsely stenotic or occluded, lowering reader scores. For saturation-prone segments such as V3, signal continuity relative to the ICA should be an endpoint, consistent with the strong associations between V3 scores and both the V3/ICA-C3 signal ratio and the proximal-to-distal decay rate.

Lowering the FA from 18° to 12° improves V3 depiction while causing no measurable loss of depiction of the other cervical vessels, whose SNR and CNR rose monotonically with FA, peaked at 25° and never showed V3's saturation-driven decline (Table 4, Fig. 5). The mild reduction in fast-flow segment SNR/CNR at 12° (e.g. ICA-C3 SNR, 504.2 to 389.3) left abundant signal, so subjective scores remained near maximal. Thus 18° buys marginally higher SNR/CNR at the cost of severe V3 saturation (43.3% adequacy), whereas 12° makes V3 uniformly diagnostic at virtually no cost; 10–14° (12° recommended) achieves both.

Reader-assessed diagnostic adequacy was only 43.3% at 18° versus 100% at 12°, so lowering the FA to 10–14° should improve continuity, reduce non-diagnostic and pseudo-stenotic readings, and increase V3 disease detection. The V3 segment is the most compression- and tortuosity-prone vertebral segment;

rotational occlusion (Bow Hunter's syndrome, C1–C2) and dissection/stenosis cause posterior-circulation ischemia [28, 29]. Non-contrast TOF-MRA avoids contrast and ionizing radiation [9, 10]. Optimizing the FA improves V3 depiction without prolonging scan time [14]; we therefore suggest lowering the FA from 18° to 10–14° (12° recommended), particularly for patients with suspected V3 disease or vertebral artery dominance, with no measurable loss of depiction of other cervical vessels.

This study has some limitations. First, it was a single-centre, single-scanner study with a limited sample size; the dominant-type subgroup comprised only 8 participants, so generalizability requires confirmation across centres, vendors and larger cohorts. Second, the 12° benefit has not yet been validated prospectively in a cohort with known V3 disease (stenosis, dissection or rotational occlusion). Finally, because TONE 70% makes the slab inflow-to-outflow angles covary with the centre FA (9.88° at inflow to 14.12° at outflow at centre FA 12°), the optimum is specific to this TONE profile and may shift under a different TONE percentage. These limitations do not alter the core conclusion that the optimal V3 FA is lower than the routine 18°, but confirmation in disease cohorts and across platforms is needed.

Conclusion

For cervical 3D TOF-MRA, lowering the FA from the routine 18° to 12° (10–14° acceptable) significantly improved reader-assessed depiction of the vertebral artery V3 segment and its reader-assessed diagnostic adequacy, without degrading the depiction of the ICA-C3 segment, the common carotid artery origin or the vertebral artery V2 segment. FA optimization for cervical TOF-MRA should be tailored to the flow characteristics of the target vessel rather than adopting the 18–20° carotid preset. Because the optimum was derived with a TONE factor of 70%, centres using a different TONE profile should re-optimize the flip angle locally.

Abbreviations

3D TOF-MRA
three dimensional time-of-flight magnetic resonance angiography
CBR
contrast-to-background muscle ratio
CI
confidence interval
CNR
contrast-to-noise ratio
FA
flip angle
ICA
internal carotid artery
IRB
institutional review board

ROI
region of interest
SI
signal intensity
SNR
signal-to-noise ratio
STROBE
Strengthening the Reporting of Observational Studies in Epidemiology
TONE
tilted optimized non-saturating excitation
VA
vertebral artery.

Declarations

Ethics approval and Consent to participate

This study was approved by the Institutional Review Board of Tingzhou Hospital (approval No. TZYY-2026-0413). All procedures were performed in accordance with the 1964 Declaration of Helsinki and its later amendments. Written informed consent was obtained from all participants.

Consent to publication

Not applicable.

Availability of data and materials

The datasets generated and analyzed during the current study are available from the corresponding author on reasonable request.

Competing interests

The authors declare that they have no competing interests.

Funding

This study received no specific funding.

Authors' contributions

Guijin Li: Study design, manuscript drafting and revision. Jiewen Qiu: Volunteer recruitment, statistical analysis. Dianjiang Zhao: Subjective image quality scoring. Hongjie Cao: Subjective image quality scoring. Xiuqin Jia: Manuscript revising and editing. Haishui Xie: Quantitative data analysis. Shuitao Qiu:

Data acquisition, image processing. Qi Yang: Overall study design, supervision, and project administration. All authors read and approved the final manuscript.

Acknowledgements

Not applicable.

References

1. Griffin KJ, Harmsen WS, Mandrekar J, Brown RD Jr., Keser Z. Epidemiology of Spontaneous Cervical Artery Dissection: Population-Based Study. Stroke. 2024;55(3):670–7.
2. Mayer-Suess L, Knoflach M, Peball T, Mangesius S, Steiger R, Pereverzyev S Jr., Lerchner H, Blache L, Mayr M, Ratzinger G, et al. Cervical Artery Tortuosity Is Associated With Dissection Occurrence and Late Recurrence: A Nested Case-Control Study. Stroke. 2025;56(2):413–9.
3. Liu J, Ning Z, Du C, Chen S, Wang T, Cao J, Huo R, Li D, Yang D, Shen R, et al. Histological validation of three-dimensional variable flip angle turbo spin echo multi-contrast magnetic resonance vessel wall imaging in characterizing carotid vulnerable atherosclerotic plaques. J Cardiovasc Magn Reson. 2024;26(2):101112.
4. Zhang C, Li Z, Liu L, Pu Y, Zou X, Yan H, Pan Y, Zhao X, Wang Y, Wang Y. Posterior circulation stroke due to vertebral artery disease in the Chinese population. Int J Stroke. 2022;17(7):753–60.
5. Koch A, Aydin OU, Hilbert A, Rieger J, Tanioka S, Ishida F, Frey D. Cross-modality image synthesis from TOF-MRA to CTA using diffusion-based models. Med Image Anal. 2025;105:103722.
6. Mou L, Lin J, Zhao Y, Liu Y, Ma S, Zhang J, Lv W, Zhou T, Liu J, Frangi AF, et al. COSTA: A Multi-Center TOF-MRA Dataset and a Style Self-Consistency Network for Cerebrovascular Segmentation. IEEE Trans Med Imaging. 2024;43(12):4442–56.
7. Koktzoglou I, Huang R, Ankenbrandt WJ, Walker MT, Edelman RR. Super-resolution head and neck MRA using deep machine learning. Magn Reson Med. 2021;86(1):335–45.
8. van Holten J, Wielopolski P, Brück E, Pattynama PMT, van Dijk LC. High flip angle imaging of metallic stents: Implications for MR angiography and intraluminal signal interpretation. Magn Reson Med. 2003;50(4):879–83.
9. Sun K, Duan C, Lou X, Shen D. MIP-Enhanced Uncertainty-Aware Network for Fast 7T Time-of-Flight MRA Reconstruction. IEEE Trans Med Imaging. 2025;44(5):2270–82.
10. Shi Z, Zhao X, Zhu S, Miao X, Zhang Y, Han S, Wang B, Zhang B, Ye X, Dai Y, et al. Time-of-Flight Intracranial MRA at 3 T versus 5 T versus 7 T: Visualization of Distal Small Cerebral Arteries. Radiology. 2023;306(1):207–17.
11. Schubert T, Pansini M, Bieri O, Stippich C, Wetzel S, Schaedelin S, von Hessling A, Santini F. Attenuation of blood flow pulsatility along the Atlas slope: a physiologic property of the distal vertebral artery? AJNR Am J Neuroradiol. 2015;36(3):562–7.

12. Saloner D. The AAPM/RSNA physics tutorial for residents. An introduction to MR angiography. Radiographics. 1995;15(2):453–65.
13. Nägele T, Klose U, Grodd W, Martos J. [MR angiography of the neck vessels with optimized linearly increasing flip angles]. Rofo. 1994;161(5):399–403.
14. Atkinson D, Brant-Zawadzki M, Gillan G, Purdy D, Laub G. Improved MR angiography: magnetization transfer suppression with variable flip angle excitation and increased resolution. Radiology. 1994;190(3):890–4.
15. von Elm E, Altman DG, Egger M, Pocock SJ, Gøtzsche PC, Vandenbroucke JP. Strengthening the Reporting of Observational Studies in Epidemiology (STROBE) statement: guidelines for reporting observational studies. BMJ. 2007;335(7624):806–8.
16. Edelman RR, Koktzoglou I. Noncontrast MR angiography: An update. J Magn Reson Imaging. 2019;49(2):355–73.
17. Wheaton AJ, Miyazaki M. Non-contrast enhanced MR angiography: Physical principles. J Magn Reson Imaging. 2012;36(2):286–304.
18. Ikushima I, Korogi. Y, Hirai. T, Takahashi M. Variable tip angle slab selection pulses for carotid and cerebral time-of-flight MR angiography. *Acta Radiologica* 1997, 38(1997)(2):275–280.
19. Fellner C, Strotzer M, Geissler A, Kohler SM, Krämer BK, Spies V, Held P, Gmeinwieser J. Renal arteries: evaluation with optimized 2D and 3D time-of-flight MR angiography. Radiology. 1995;196 3:681–7.
20. Dagirmanjian A, Ross JS, Obuchowski N, Lewin JS, Tkach JA, Ruggieri PM, Masaryk TJ. High resolution, magnetization transfer saturation, variable flip angle, time-of-flight MRA in the detection of intracranial vascular stenoses. J Comput Assist Tomogr. 1995;19(5):700–6.
21. Jiang Y, Gu H, Cai Z, Fu S, Cao Y, Jiang L, Wu C, Chen W, Xia C, Lui S, et al. Ultra-small manganese dioxide nanoparticles with high T(1) relaxivity for magnetic resonance angiography. Biomater Sci. 2023;11(12):4359–69.
22. Mizoshiri T, Yoshida M, Oda S, Tsumagari S, Nakaura T, Harada K, Ikeda O. Non-contrast mDixon MR angiography of the neck: Comparison with time-of-flight MR angiography in normal subjects. Medicine. 2021;100:e28351.
23. Bowen BC. MR Angiography versus CT Angiography in the Evaluation of Neurovascular Disease. Radiology. 2007;245(2):357–61.
24. Lu H, Clingman C, Golay X, van Zijl PC. Determining the longitudinal relaxation time (T1) of blood at 3.0 Tesla. Magn Reson Med. 2004;52(3):679–82.
25. Frahm J, Haase A, Matthaei D. Rapid NMR imaging of dynamic processes using the FLASII technique. Magn Reson Med. 1986;3(2):321–7.
26. Ernst RR, Anderson WA. Application of Fourier Transform Spectroscopy to Magnetic Resonance. Rev Sci Instrum. 1966;37(1):93–102.

27. Shimada K, Nagasaka T, Shidahara M, Machida Y, Tamura H. In vivo measurement of longitudinal relaxation time of human blood by inversion-recovery fast gradient-echo MR imaging at 3T. Magn Reson Med Sci. 2012;11(4):265–71.
28. Duan G, Xu J, Shi J, Cao Y. Advances in the Pathogenesis, Diagnosis and Treatment of Bow Hunter's Syndrome: A Comprehensive Review of the Literature. Interventional Neurol. 2016;5(1–2):29–38.
29. Zaidi HA, Albuquerque FC, Chowdhry SA, Zabramski JM, Ducruet AF, Spetzler RF. Diagnosis and management of bow hunter's syndrome: 15-year experience at barrow neurological institute. World Neurosurg. 2014;82(5):733–8.

Figures

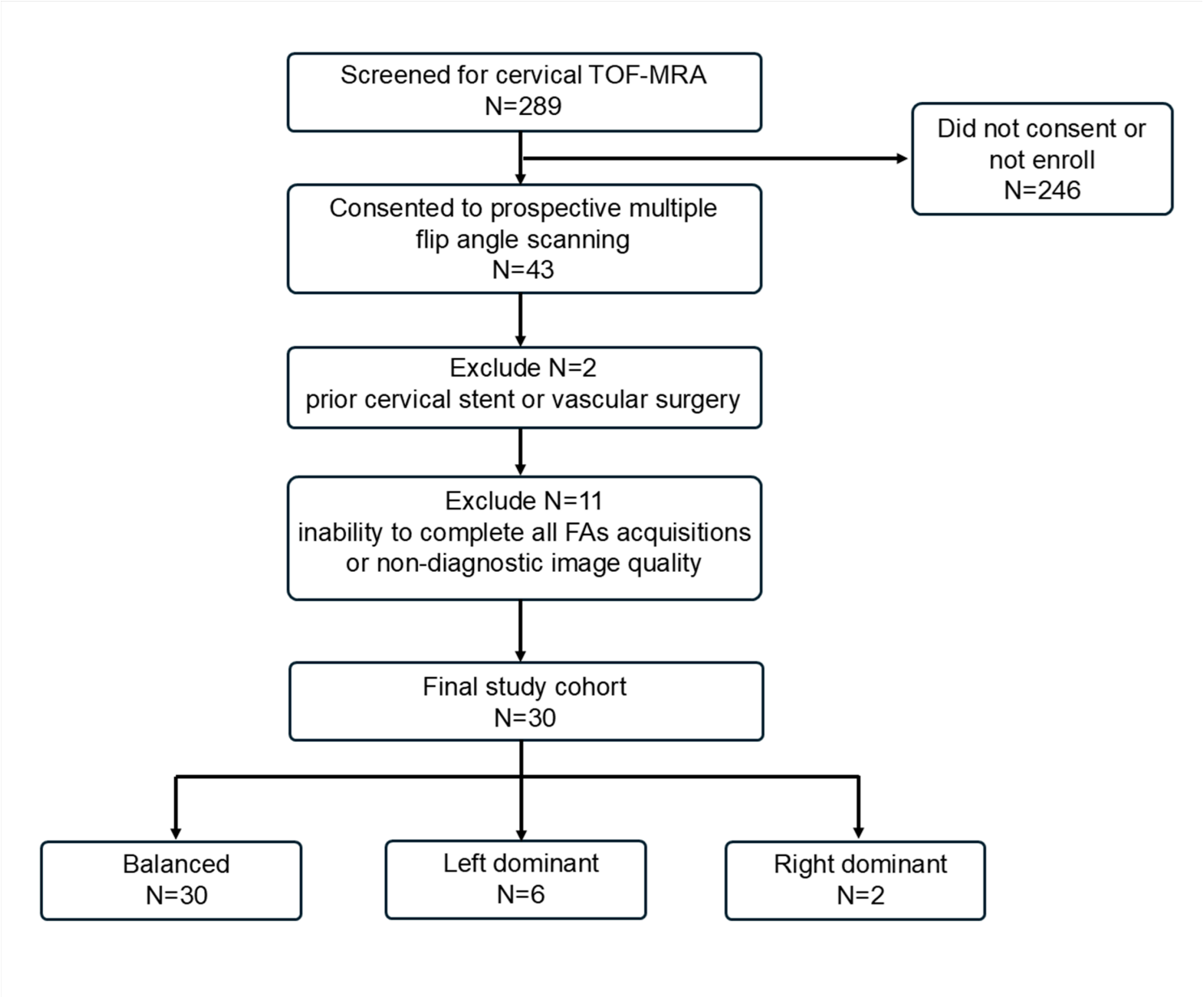


Figure 1

Study flowchart, from initial screening to the final study cohort. The cohort is further divided according to vertebral artery dominance.

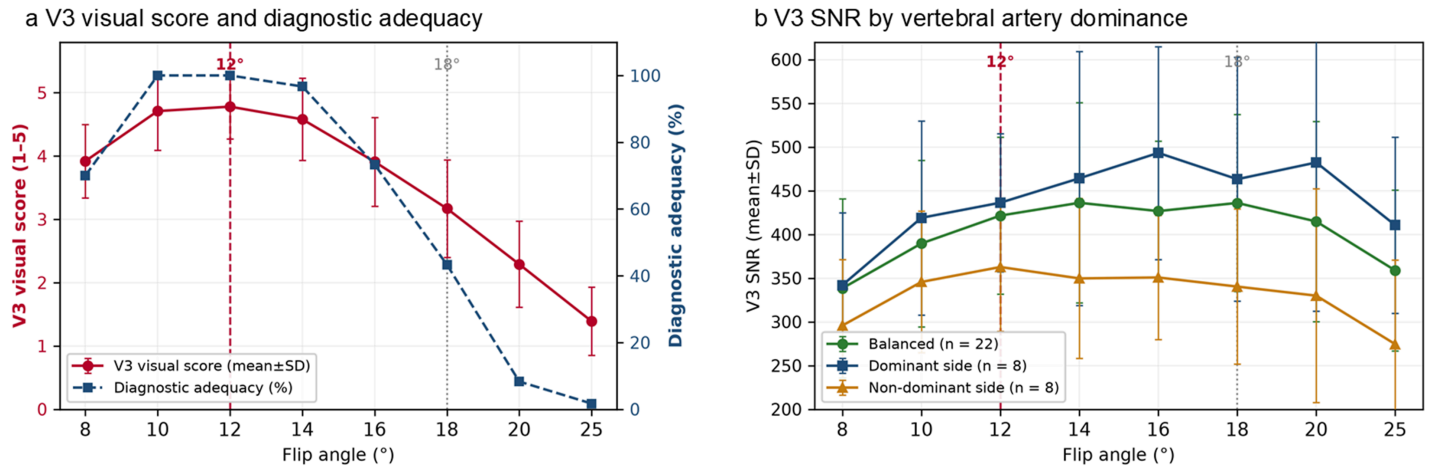


Figure 2

V3 segment depiction as a function of FA (n = 30). a V3 visual score (mean ± SD, left axis) and reader-assessed diagnostic adequacy (%, right axis). b V3 SNR (mean ± SD) stratified by vertebral artery dominance (balanced, dominant side and non-dominant side). The red dashed line marks the optimal FA of 12°; the grey dotted line marks the routine 18°.

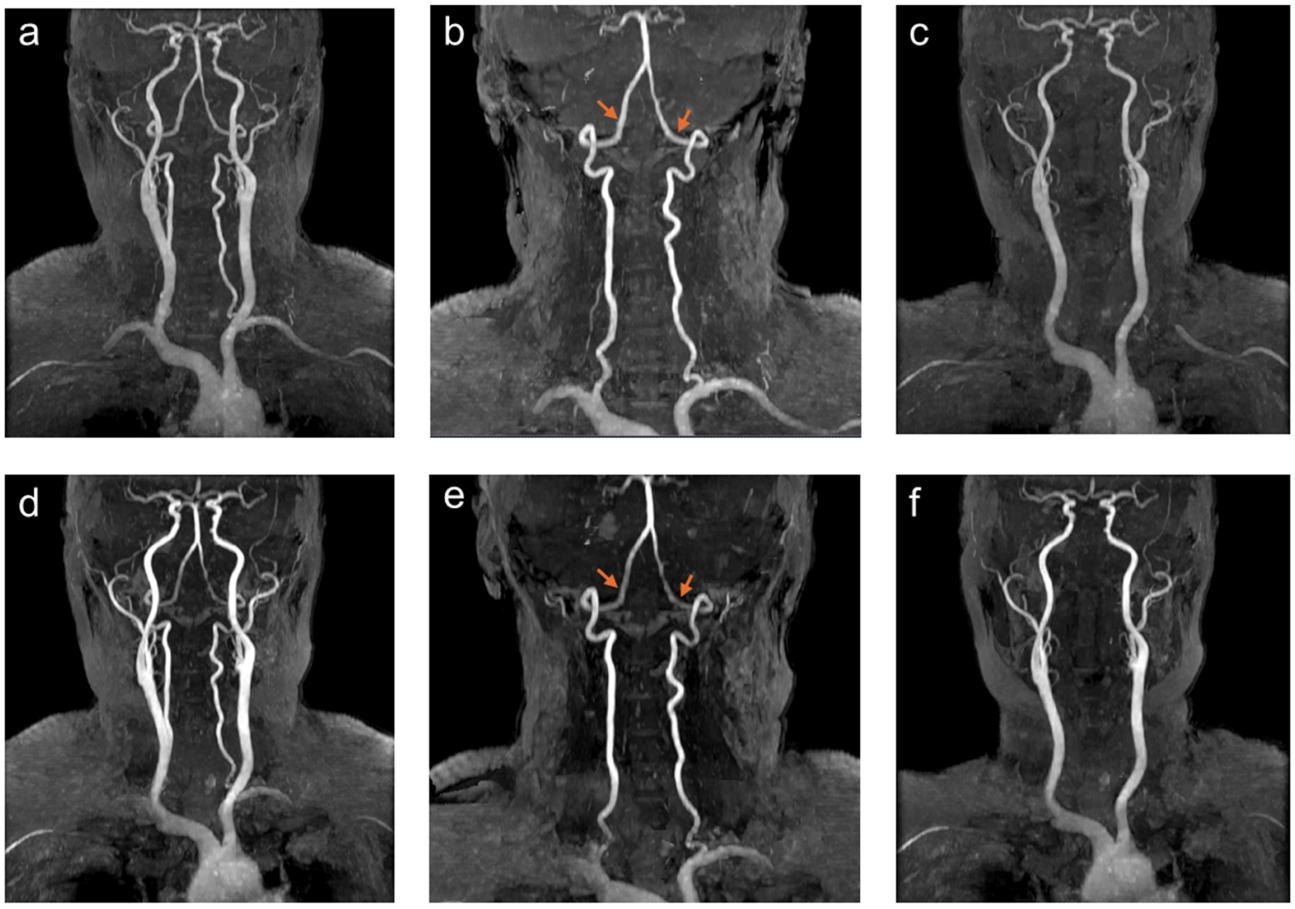


Figure 3

MIP images of the cervical vessels acquired at a centre FA of 12° (a–c) and 18° (d–f). a–c Images at 12°: a global view of the cervical vessels, b vertebral artery and c carotid artery images. d–f Corresponding images at 18°. Compared with 18°, the 12° acquisition shows more complete depiction of the vertebral artery V3 segment (orange arrow) and less in-slab signal loss, in keeping with the quantitative results above.

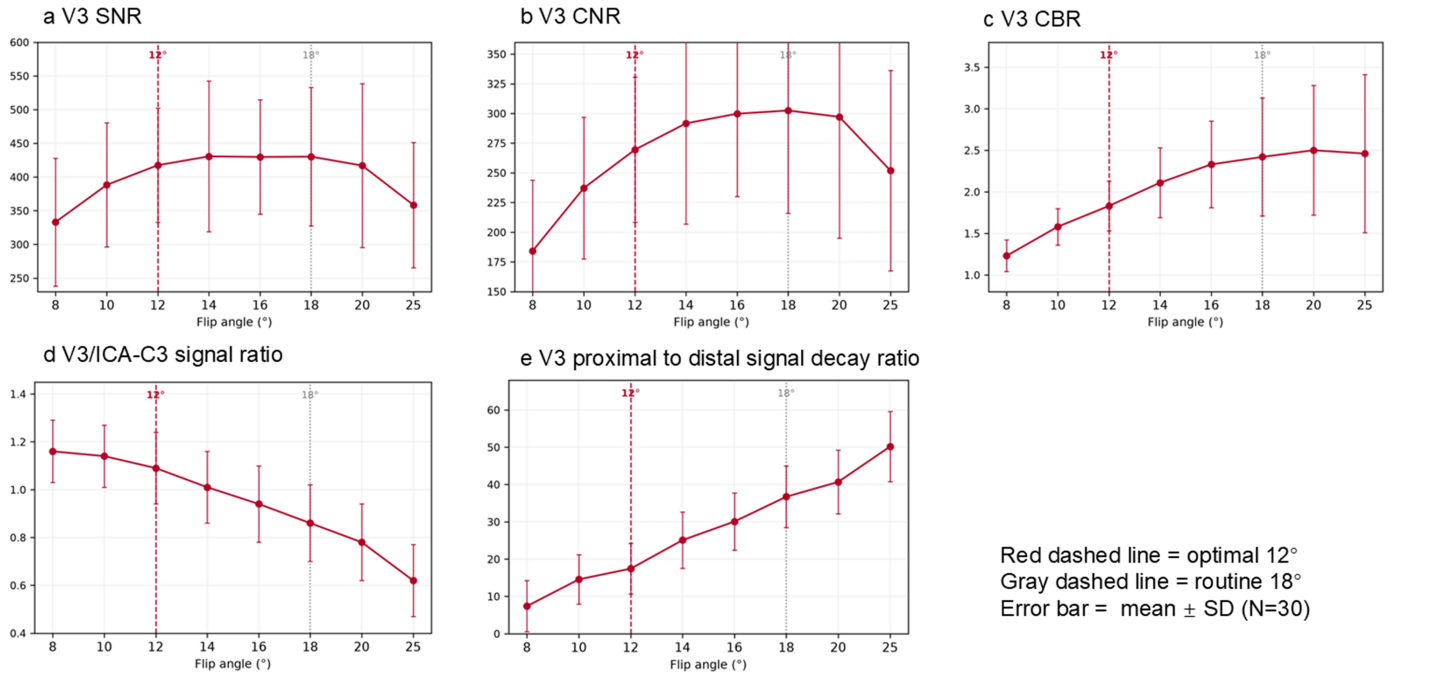


Figure 4

V3 segment quantitative metrics versus FA (n = 30): a SNR, b CNR, c CBR, d V3/ICA-C3 signal ratio and e proximal-to-distal decay rate. Error bars indicate mean ± SD; the red dashed line marks 12° and the grey dotted line 18°. CBR, contrast-to-background ratio; CNR, contrast-to-noise ratio; ICA, internal carotid artery; SNR, signal-to-noise ratio.

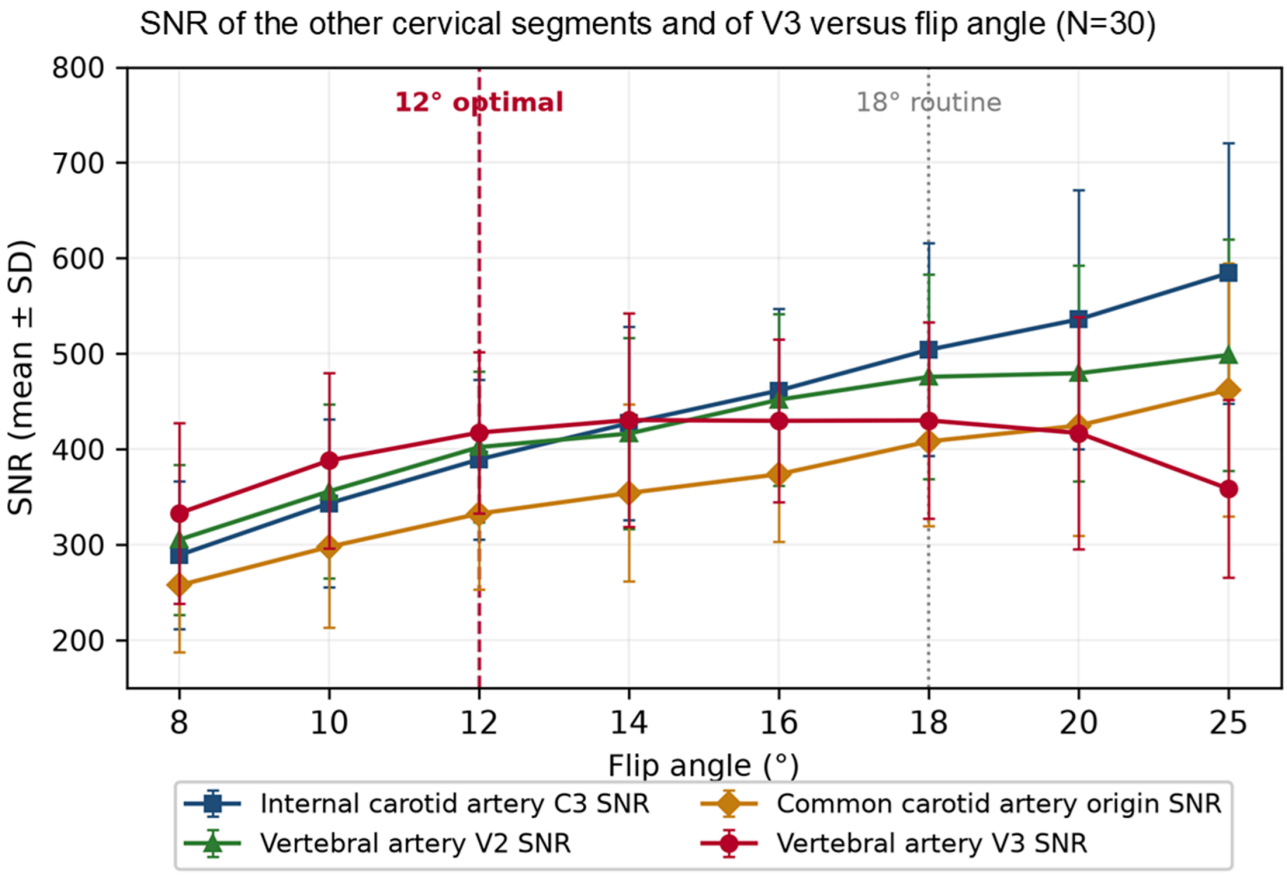


Figure 5

SNR of the other cervical segments and of the vertebral artery V3 segment as a function of FA (n = 30). The SNR of the internal carotid artery C3 segment, the vertebral artery V2 segment and the common carotid artery origin increases monotonically with FA, whereas V3 shows an inverted U. The red dashed line marks the optimal 12° and the grey dotted line the routine 18°.